ARMA 21–21

Multi-Layer Reservoir Thermal Energy Storage in the Uinta Basin

Palash Panja
Department of Chemical Engineering, University of Utah, Salt Lake City, Utah, USA
Energy & Geoscience Institute, University of Utah, Salt Lake City, Utah, USA
Sídney Green
Enhanced Production, Inc., Salt Lake City, Utah, USA
Research Professor, University of Utah, Salt Lake City, Utah, USA
Milind Deo
Department of Chemical Engineering, University of Utah, Salt Lake City, Utah, USA
Richard Allis
Consultant, Salt Lake City, Utah, USA
Richard Newhart
Consultant, Denver, Colorado, USA
Kevin Kitz
KitzWorks LLC, Boise, Idaho, USA
Joseph Moore
Energy & Geoscience Institute, University of Utah, Salt Lake City, Utah, USA
John McLennan
Department of Chemical Engineering, University of Utah, Salt Lake City, Utah, USA
Energy & Geoscience Institute, University of Utah, Salt Lake City, Utah, USA

Copyright 2021 ARMA, American Rock Mechanics Association

This paper was prepared for presentation at the 55th US Rock Mechanics/Geomechanics Symposium held in Houston, Texas, USA, 20-23 June 2021. This paper was selected for presentation at the symposium by an ARMA Technical Program Committee based on a technical and critical review of the paper by a minimum of two technical reviewers. The material, as presented, does not necessarily reflect any position of ARMA, its officers, or members. Electronic reproduction, distribution, or storage of any part of this paper for commercial purposes without the written consent of ARMA is prohibited. Permission to reproduce in print is restricted to an abstract of not more than 200 words; illustrations may not be copied. The abstract must contain conspicuous acknowledgement of where and by whom the paper was presented.

ABSTRACT:

Reservoir thermal energy storage ("RTES") in high porosity and high permeability sedimentary settings offers the potential for large-scale and long-term heat energy storage for future any-time electricity production. Solar-generated thermal energy or excess solar or wind electricity are expended to heat water on the surface and is subsequently injected into adequately deep, porous formations. Three numerical models with single layer, two layers and four layers of high permeability (100mD) and high porosity (15%) separated by thinner layer (s) of low permeability (1mD) and low porosity (5%) are developed for potential multi-layer subsurface hot water storage reservoirs mimicking the Uinta Basin. Three operational scenarios are studied: in scenario1, hot water is injected for 8 hrs. per day (40kg/s) without production; in scenario2, the daily cycle is operated as 8 hrs. of injection (40kg/s), 10 hrs. of production (32kg/s) and 6 hrs. of shut-in; scenario3 is the combination of scenarios 1 and 2 where water is only injected (scenario1) for 30 days first and then daily cycle (scenario2) is continued. Issues considered include conformance (uniform injection and production over the multi-layers), thermal stratification, and heat loss; all requiring multi-layer calculations. Simulation results are discussed with conclusions presented for the optimization of multi-layer RTES applications in the Uinta Basin.

1. INTRODUCTION

The importance of large-scale and long-term energy storage is clearly shown as the rapid adoption of solar and wind electrical generation proceeds (DOE 2020). Such storage is essential to effectively manage the intermittent nature of solar and wind (Green 2020, Andreas et al. 2021). Already, vast amounts of renewable solar and wind electricity are being curtailed. This is nearly free renewable electricity. Also, substantial solar and wind facilities are under construction and/or being planned. Energy storage has become the primary enabling technology to further implement solar and wind electric power generation worldwide (Agarwal and Giberti 2020, Morgan 2020).

Recent research has shown the potential of reservoir thermal energy storage ("RTES") for deep subsurface storage of water at high temperature; 250°C, for example. Practical recovery of almost all of the stored heat is possible for long-term or seasonal storage (Panja et al. 2020, Panja et al. 2021). Research has also shown that electricity costs anticipated from RTES geothermal electricity production can be competitive with conventional geothermal electricity (Wendt et al. 2019,

Downloaded from http://onepetro.org/ARMAUSRMS/proceedings-pdf/ARMA21/All-ARMA21/2499885/arma-2021-0021.pdf by The University of Utah user on 20 October 2021

Sharan et al. 2020) and potentially much lower depending on the reservoir storage exploration and construction costs[10]. As one form of RTES, Geothermal Battery Energy Storage ("GB") has previously been described in the literature (McLennan and Green 2020, McLennan et al. 2020, Green et al. 2021). One of the challenges in the overall design of the GB system is to mitigate wellbore and, surface scaling and permeability reduction in the reservoir due to the geochemical behavior of produced and injected water.

GB creates localized geothermal reservoirs using either solar-generated thermal energy or excess solar or wind electricity. These energy sources are used to heat water on the surface facility. The heated water is subsequently injected into adequately deep, porous formations (Green et al. 2021). Previously published calculations have shown subsurface heat and fluid flow for different injection and withdrawal scenarios (Panja et al. 2020, Panja et al. 2021). These calculations have shown the high efficiency in terms of heat injected to practical heat extracted.

Ideally, a single vertically extensive and homogeneous porous zone is desired. However, practically two or three thinner layers overlying each other will be more common in realistic geologic scenarios. We have studied the multi-layer reservoir as a potential RTES in the present work. Researchers (Dubiel 2003, Birgenheier and Berg 2011, Sprinkel 2016) have described major stratigraphic units in the Uinta basin from core samples, outcrop mapping and well logs. This stratigraphy reveals a stacking pattern of multiple layers. To study the GB potential in the Uinta basin, two simplified reservoir models (two-layer, and four-layer) are developed. Additionally, a single layer model is also developed for comparison. Three operational scenarios are studied in these three reservoir models.

Spatial distributions of temperature for all cases are shown. Variations of bottom hole temperature and pressure with injection/production cycles are also shown. Cumulative heat recovered while varying the number of cycles of injection-production for selected operational cases is also discussed.

The coupled thermal and fluid flows, including convective and conductive heat flow, are numerically calculated using a commercial thermal simulator STARS from the Computer Modeling Group (CMG, Calgary, Canada).

2. RESERVOIR MODEL AND SIMULATION

To investigate thermal energy storage in multi-layer formations, three reservoirs are studied: a single layer, two layers, and four layers, as shown in Figure 1 a, b, and c, respectively.

The simulated reservoir has the dimensions of 200 meters in the x-, 200 meters in the y-, and 175 meters in the z-directions. The reservoir is divided into 4 (3 for the single layer) parts; overburden, basal rock, permeable layer in the middle, and intermediate layers separating permeable layers in case of two- and four-layer models. The permeable layer(s)' total thickness is fixed at 60 meters for all models, i.e., one layer of 60 meters for the single-layer model, two layers of 30 meters for the two-layer model, and four layers 15 meters for the four-layers model. These permeable layers have 100 mD permeability and 15% porosity. Relatively low permeability layers are located between two permeable layers for the two- and four-layer models. The permeability and porosity of these intermediate layers are 1 mD and 5%, with a total thickness of 15 m (one 15 meters for the two-layer model and three 5 meters layers for the four-layer model). The thickness of the overburden and basal rock is 57.5 meters each for the single-layer model and 50 meters each for the two- and four-layer models. The permeability and porosity of the overburden and basal rock are 0.01 mD and 3%. The well has perforations in all permeable and intermediate layers. The

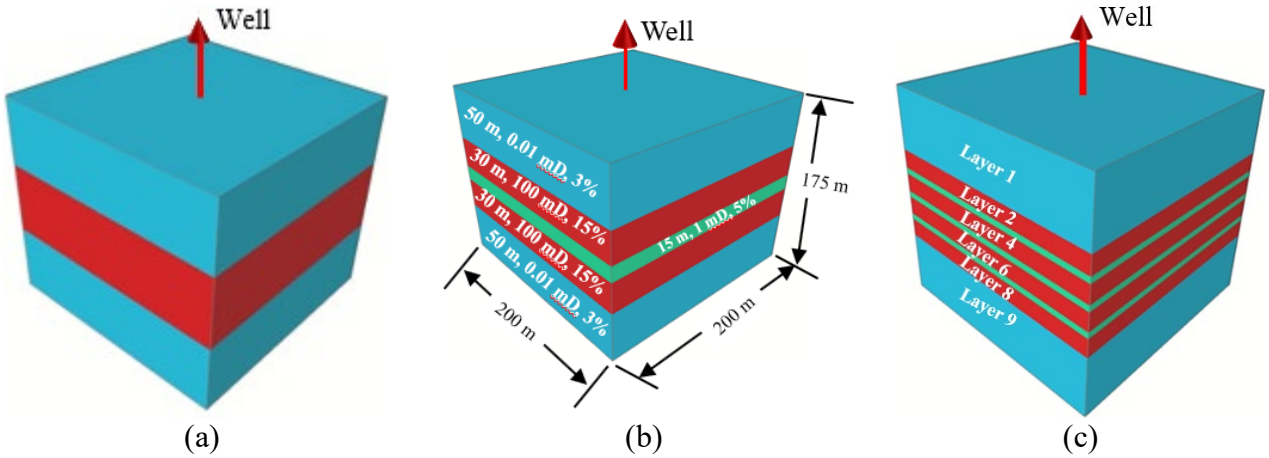

Fig. 1. Three different reservoirs configurations consisting of (a) one permeable layer, (b) two permeable layers (c) four permeable layers

Downloaded from http://onepetro.org/ARMAUSRMS/proceedings-pdf/ARMA21/All-ARMA21/2499885/arma-2021-0021.pdf by The University of Utah user on 20 October 2021

reference temperature and pressure at the middle of the reservoirs are 120^{O}C, and 18.5 MPa, respectively, and they are varied with height with gradients of 35^{O}C/km and 10.5 MPa/km.

Three different operational scenarios are studied for each of the three reservoir models. To investigate long-term geothermal storage, hot water at 250^{O}C is injected at 40 kg/second for 8 hours per day, and the well is kept shut-in for the rest of the day (16 hours), as shown in Figure 2(a). This operation is continued for four months. In the second operational scenario, water -at the same conditions - is injected at 40 kg/second for 8 hours per day, and then production is started at 32 kg/second for 10 hours per day, and then well is shut-in for 6 hours, as shown in Figure 2(b).

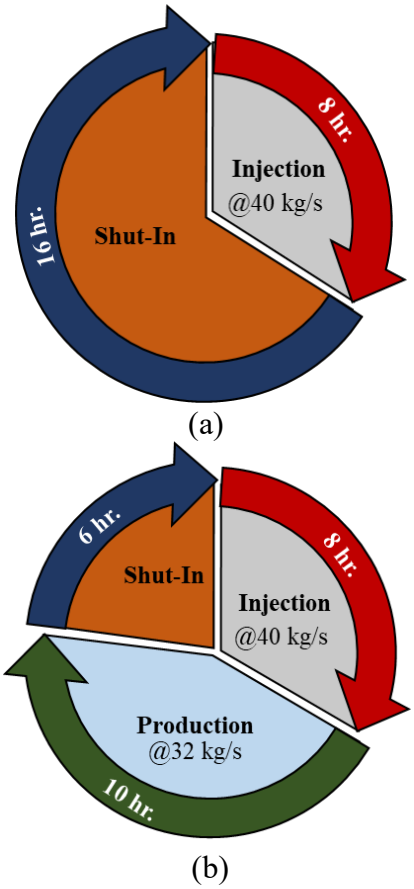

Fig. 2. Two operational scenarios of geothermal heat storage and production (a) injection and shut-in only (b) daily cycle of injection, production, and shut-in

The third operational scenario is a combination of the first two where only injection (1st scenario) is carried out for one month. This can be considered as charging of the reservoir or seasonal or temporary storage only. After that, the daily cycle (2nd scenario) is started and continued.

3. RESULTS

The impacts of layering and operational strategies are investigated by analyzing spatial distributions of temperature in the reservoir, bottom hole temperature, bottom hole pressure, and heat recovery. We have plotted the average bottom hole temperature and pressure changes with time (or cycle). The results are discussed for four months, i.e., 120 operating cycles (equivalent to 120 days of operation.

3.1. HEAT STORAGE ONLY (SCENARIO 1)

Figure 2a shows operational scenario 1, which is intended for heat storage purposes only. The hot water distributions in the reservoir after 1 month and 4 months of injection are shown in figure 3 for three geologic settings. As more water is injected into the formation without production, the hot and cold water interface moves farther from the wellbore. In the single-layer model, it travels about 25 meters over 1 month and 50 meters over 4 months. These results are supported by our previous study for a single-layer homogeneous reservoir (Green et al. 2021). The radius of the hot water front is proportional to the square root of the volume injected, assuming cylindrical movement of the hot water. Hence, we expect that the mixing front travels twice the distance in 4 months that it travels in 1 month. Therefore, the results confirm that the heat loss to the surroundings is not significant with time. Most of the heat is conserved in the hot water zone.

The results are not significantly different for the two-layer and four-layer models, although some water invades the intermediate layers. This is because the target formation has significantly higher permeability and porosity compared to the intermediate layers. Consequently, the amount of hot water going to the intermediate layers is negligible compared to the water injected in the formation layers. The overburden and basal rock also play a role in minimizing any heat losses. However, 3 meters (after 1 month) to 7 meters (after 4 months) of overburden and basal rock are slightly heated which can be considered as heat loss. This heat is transferred mainly by conduction through rock and not by the water flow due to the very low permeability (0.01 mD) and porosity (3%) of these segments.

The average bottom hole pressures for the three models are plotted for a 120-day operational cycle in figure 4. The bottom hole pressure increases the number of the cycle as expected. The upper sides of the curves are the pressure during injection, and the lower sides are the shut-in pressure. As more water is injected without production, injection pressure increases. However, the constant pressure boundary condition causes the formation to return to near the initial formation pressure quickly. Also, 16 hours of shut-in is enough time for pressure stabilization. The increase in injection pressure depends on the compressibility and thermal expansion of both the rock and the water.

The first ten cycles and the last ten cycles are shown in figures 4 b and c for clarity. No significant differences are found in bottom hole pressure for the different reservoir models. The reason is that the same amount of water is

Downloaded from http://onepetro.org/ARMAUSRMS/proceedings-pdf/ARMA21/All-ARMA21/2499885/arma-2021-0021.pdf by The University of Utah user on 20 October 2021

injected over the same thickness of permeable layer(s). Slight differences may be caused by injection into the intermediate layer. 2 to 2.5 MPa of pressure (i.e., the difference between pressures during injection and shut-in) is required to pump water at 40 kg/s in this formation. This value changes with operational strategy, water rate and temperature, and formation properties such as permeability and porosity. This pumping cost can be reduced by choosing a thermal energy storage reservoir with higher permeability and porosity layers.

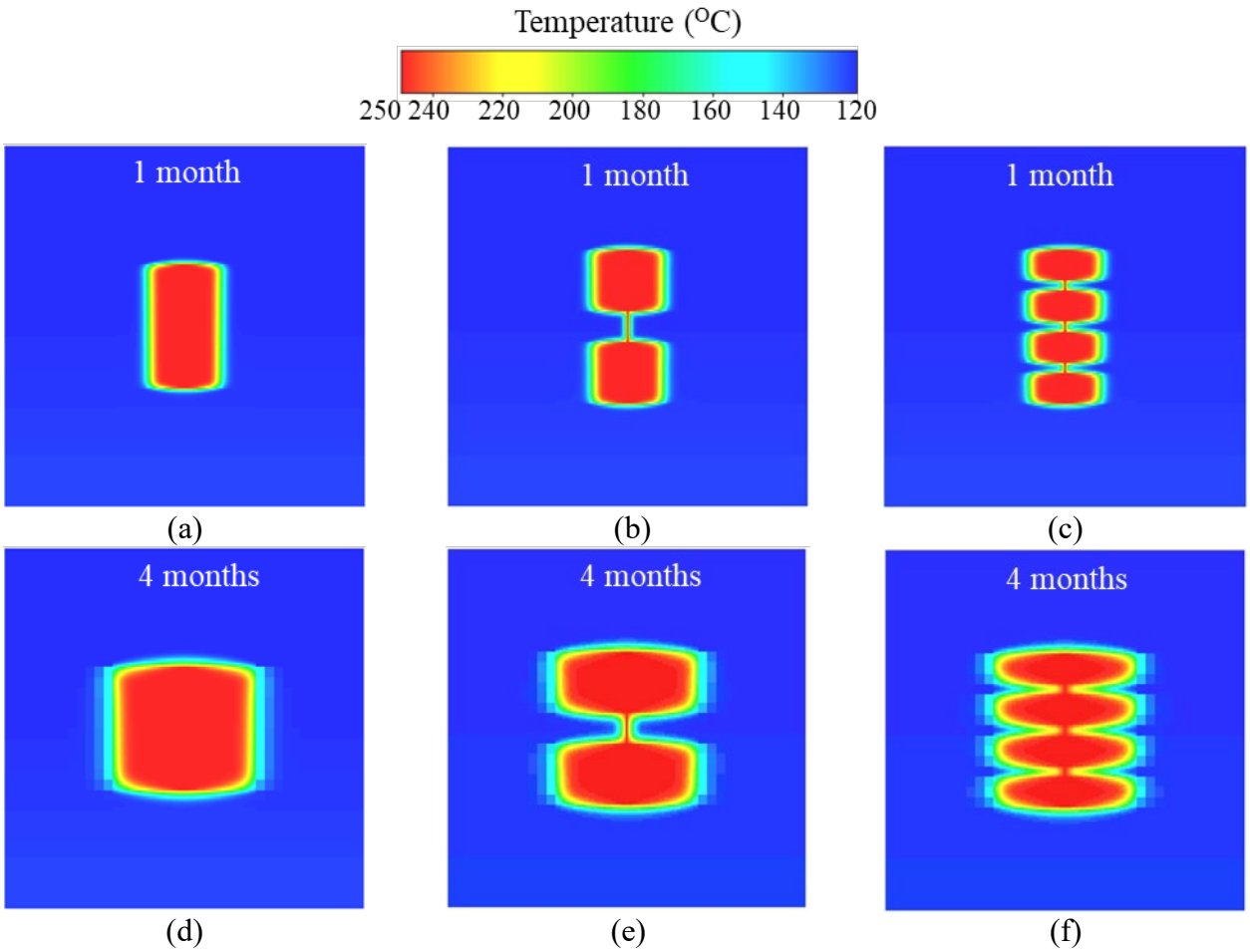

Fig. 3. Spatial distributions of temperature on the vertical, x-z plane (200 m x 175 m view) at the mid-width (middle in the y-direction) of the formation for the 1st operational scenario at the end of injection cycle of (a) 1 month in the single-layer model (b) 1 month in the two-layer model (c) 1 month in the four-layer model (d) 4 months in the single-layer model (e) 4 months in the two-layer model (f) 4 months in the four-layer model

Downloaded from http://onepetro.org/ARMAUSRMS/proceedings-pdf/ARMA21/All-ARMA21/2499885/arma-2021-0021.pdf by The University of Utah user on 20 October 2021

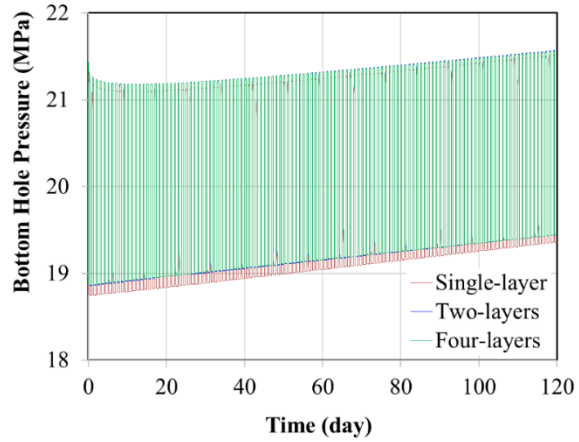

(a)

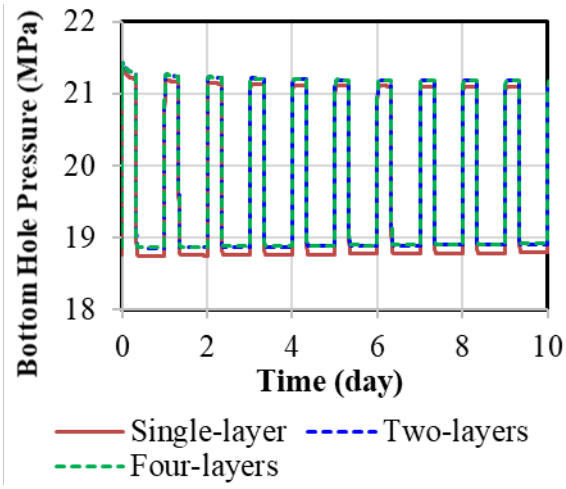

(b)

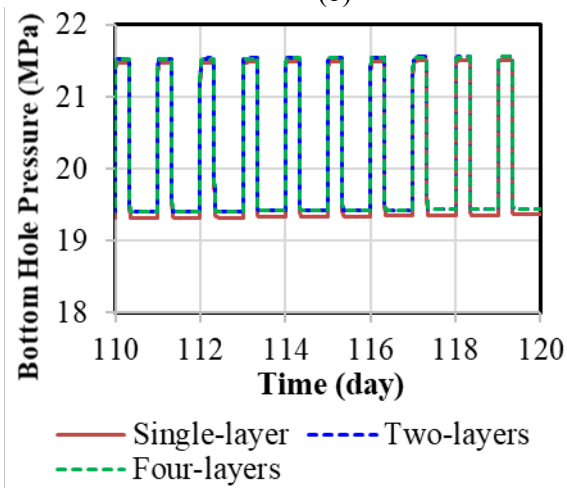

(c)

Fig. 4. Average bottom hole pressure for the 1st operational scenario (a) 4-months or 120 days (b) first 10 days (c) last 10 days

3.2. DAILY CYCLE (SCENARIO 2)

The daily operational strategy described is useful for daily power generation for 10 hours per day. This schedule fulfills the demand for electricity or heating requirements when wind and solar are not available, as during the nighttime. We have plotted temperature distribution, bottom hole temperature, bottom hole pressure, and heat recovery. The spatial distributions of temperatures in three geologic models after four months of injection are shown in figure 5.

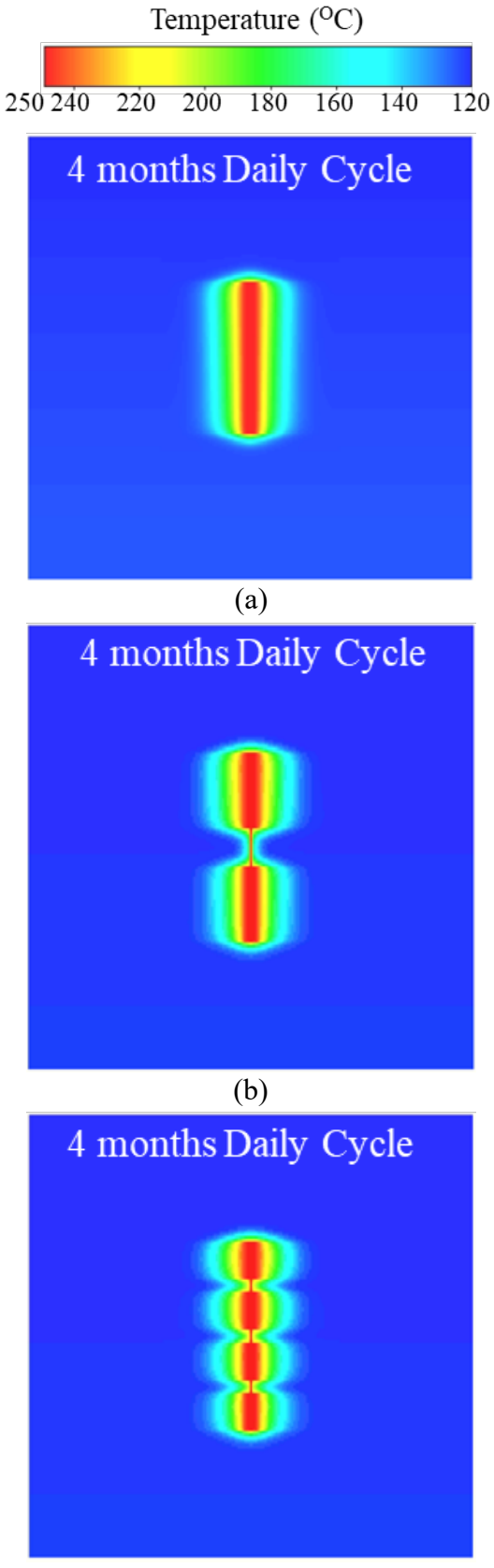

(a)

(b)

(c)

Fig. 5. Spatial distributions of temperature on the x-z plane (200 m x 175 m view) at the mid-width (middle in the y-direction)

Downloaded from http://onepetro.org/ARMAUSRMS/proceedings-pdf/ARMA21/All-ARMA21/2499885/arma-2021-0021.pdf by The University of Utah user on 20 October 2021

of the formation for the second operational scenario at the end of the injection cycles for (a) 4 months in the single-layer model (b) 4 months in the two-layer model (c) 4 months in the four-layer model.

A constant temperature zone with a radius of 4 -5 meters develops near the wellbore over time in the daily cycle of injection, production, and shut-in. Beyond this constant temperature zone of 250^{O}C (injection water temperature), temperature progressively decreases towards the initial formation temperature. A mixing front is located about 20 meters away from the wellbore after 120 days of daily cycling.

Variations of the average bottom hole temperature in the three geologic models are plotted in figure 6. The upper extremities of the curves are the temperatures during injection, whereas the lower limits are the temperatures during 6 hours of shut-in. The temperature during production steadily decreases from the injection temperature to a lower value and stays nominally constant there during shut-in.

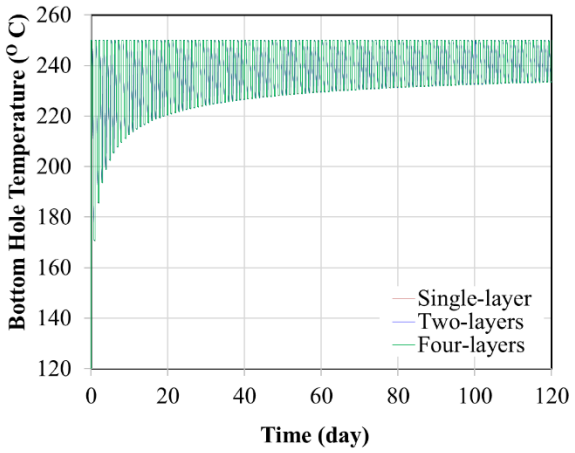

(a)

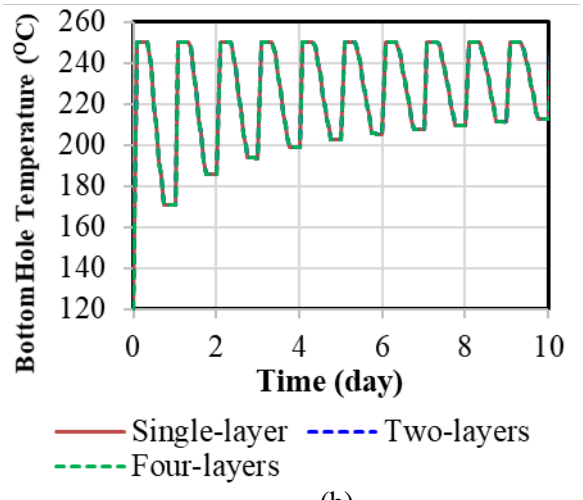

(b)

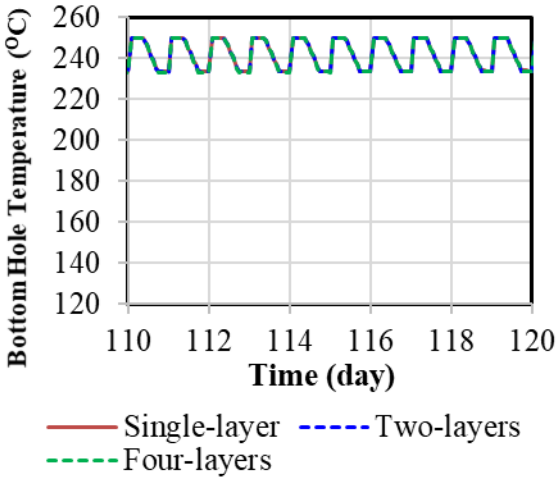

(c)

Fig. 6. Average bottom hole temperature for the second operational scenario (a) 4-months or 120 days (b) first 10 days (c) last 10 days

As observed in figure 6a the bottom hole temperature increases at the end of production with each cycle. The production temperature drops from the injected water temperature (250^{O}C) due to the heating of the surrounding rock by conduction and the mixing of injected hot water with relative cold in-situ water of 120^{O}C. As would be expected, the more significant differences between injection and production temperature are observed in the first 5-10 cycles for all of the geologic models. As the near-wellbore rock is heated and the driver for heat transfer (i.e., the temperature difference) between the water and rock becomes small, the production temperature reaches a steady value of about 235 ^{O}C after 90 cycles (see figure 6b for the last ten cycles). The production temperature never reaches the injection water temperature due to the slow heat conduction and mixing with in-situ water. The bottom hole pressures for all three models are shown in figure 7.

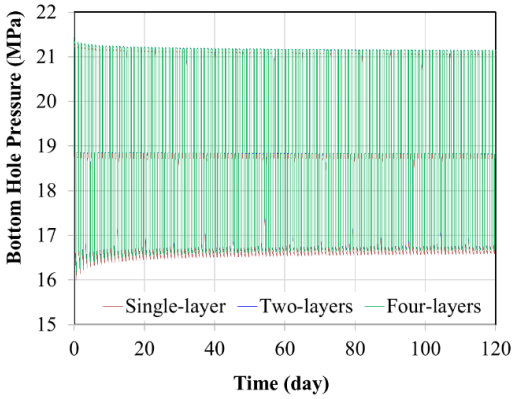

(a)

Downloaded from http://onepetro.org/ARMAUSRMS/proceedings-pdf/ARMA21/All-ARMA21/2499885/arma-2021-0021.pdf by The University of Utah user on 20 October 2021

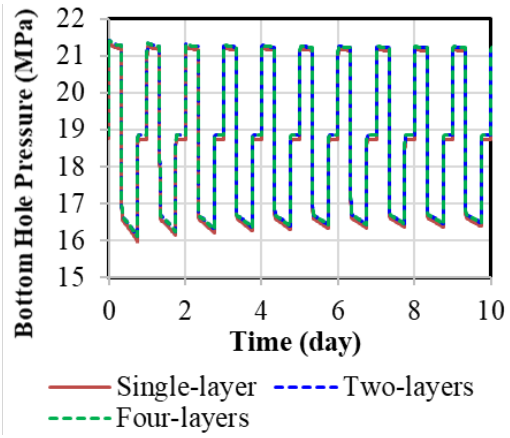

(b)

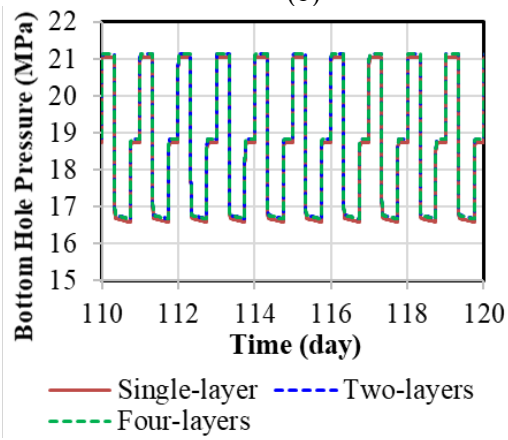

(c)

Fig. 7. Average bottom hole pressure for t operational scenario (a) 4-months or 120 days (b) first 10 days (c) last 10 days

The injection pressure is a little over 21 MPa for injecting hot water at 40 kg/s, whereas the initial reservoir pressure at the middle of the formation is 18.5 MPa. Therefore, a 2.5 MPa pressure differential is applied for the required amount of injection. Similarly, during production, pressure decreases to about 16.2 MPa, i.e., an average 2.3 MPa drawdown is applied to produce water at 32 kg/s. During shut-in, the pressure quickly reaches reservoir pressure. One reason for the quick pressure equilibration is the high porosity and permeability of the reservoir. The second reason is the constant pressure boundary condition used in the calculations. Like bottom hole temperature, bottom hole pressures are also not affected by the geologic layering when all other parameters are the same.

Cumulative heat recoveries are plotted for 120 days of operation in Figure 8. The recovery in the first cycle is only about 81% due to the heat loss for heating the formation rock and mixing with in-situ water.

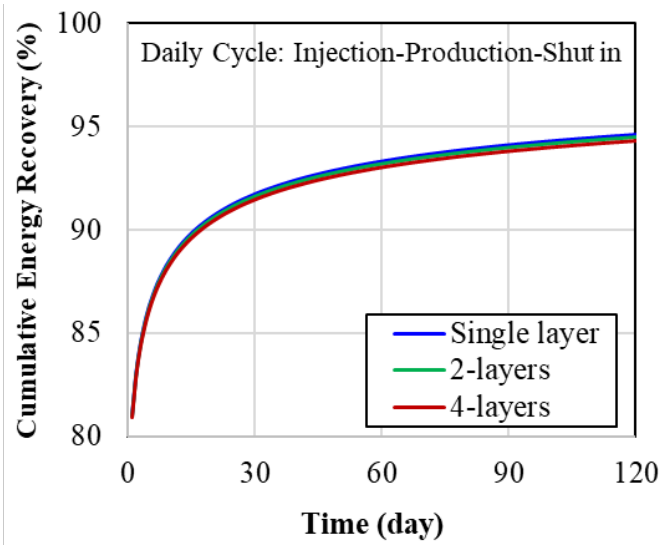

Fig. 8. Cumulative energy recovery with the number of cycles (or days) for different geologic models and 2nd operational scenario

Initially, energy recovery increases rapidly and then reaches an asymptotic nature after a few cycles. At the end of 120 days, the recovery is close to 95%. The combination of higher produced water temperature and this high recovery factor are critical factors for successfully implementing the geothermal battery energy storage in layered formations.

3.3. DAILY CYCLE AFTER INITIAL CHARGING (SCENARIO 3)

This operational scenario is intended to investigate the effect of initially charging the reservoir with hot water at 250^{O}C. This serves many purposes, such as preparing the GB for commercial operation, filling up pore space in partially saturated formations, and minimizing heat loss during the daily cycle. The temperature distributions after 1 month of injection followed by 4 months of daily cyclic injection, production, and shut-in are shown in figure 9.

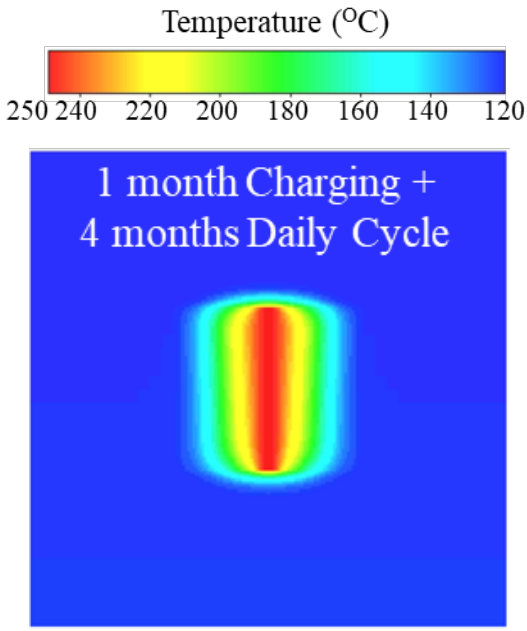

Downloaded from http://onepetro.org/ARMAUSRMS/proceedings-pdf/ARMA21/All-ARMA21/2499885/arma-2021-0021.pdf by The University of Utah user on 20 October 2021

(a)

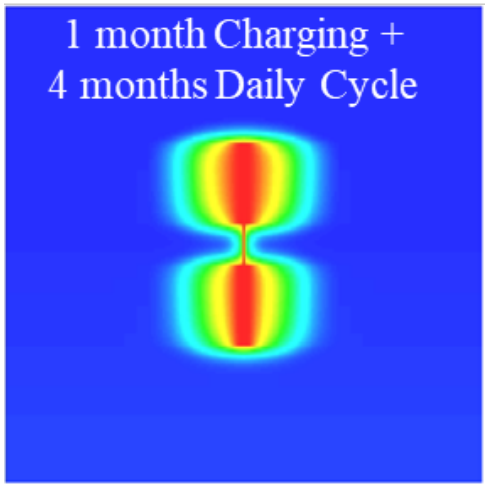

(b)

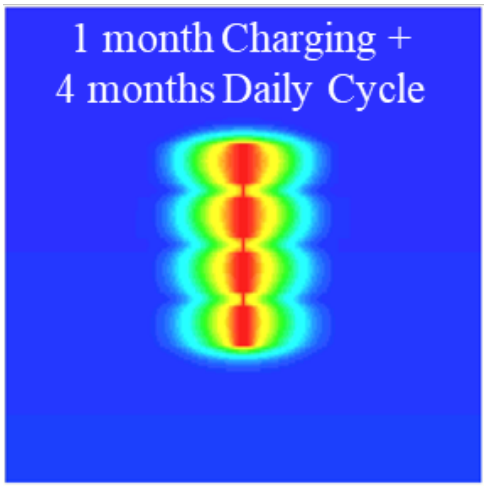

(c)

Fig. 9. Spatial distributions of temperature on the x-z plane (200 m x 175 m view) at the mid-width (middle in the y-direction) of the formation for 3rd operational scenario (1 month of injection and 4 months of daily cycling) at the end of the injection cycle in (a) single-layer model (b) two-layer model (c) four-layer model

The distributions are quite similar to those in Figure 5 where the reservoirs were not initially charged. The differences include an approximately 8-9 meters radius of the constant temperature zone and 32 meters to the mixing front. A more significant high-temperature zone is developed due to the initial injection of hot water without production for a month.

The bottom hole temperatures are plotted in figure 10.

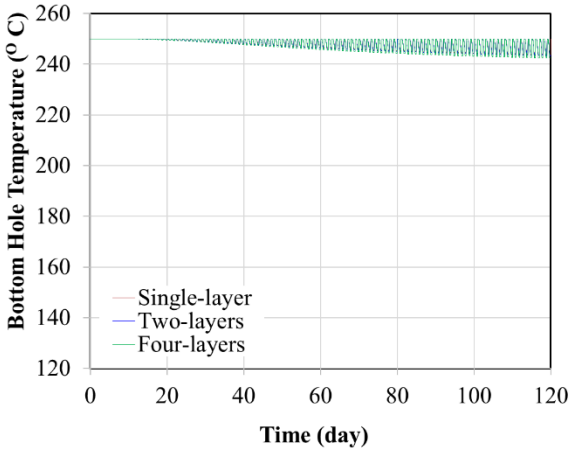

Fig. 10. Average bottom hole temperature for the third operational scenario

The initial charging improves the produced water temperature. In the first 20 cycles, the water is produced at 250°C, which implies that the injected water stored near the wellbore during charging is produced. Even in the long term, up to 120 days as studied, the produced water temperature only drops 7-8 °C. Therefore, charging the reservoir for a few days before starting a commercial operation has the great advantage of elevating the produced water temperature. However, this is achieved at the cost of one month's hot water and operation without any production. Therefore, the heat recovery factor during this time is zero, as shown in Figure 11.

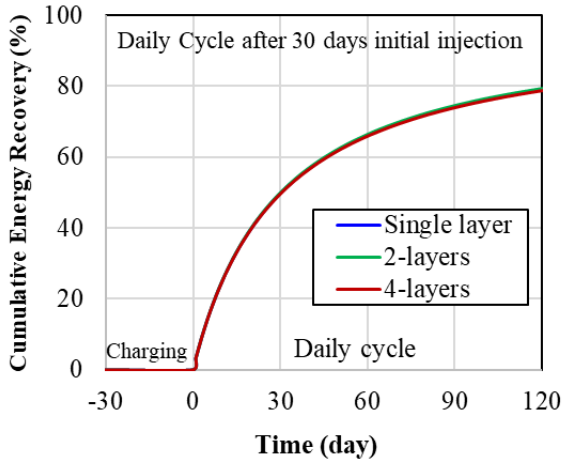

Fig. 11. Cumulative energy recovery with the number of cycles (or days) for different geologic models and 3rd operational scenario

Considering the heat injected during charging, the cumulative heat recovery during the daily cycle starts from zero and slowly picks up to a moderate value. 50% of the heat is recovered in a month and 80% after 120 days.

4. *DISCUSSION OF RESULTS*

Reservoir temperature and pressure profiles are radially symmetrical for the calculations shown - which consider only radially isotropic permeabilities. Previous calculations have considered non-isotropic permeabilities

Downloaded from http://onepetro.org/ARMAUSRMS/proceedings-pdf/ARMA21/All-ARMA21/2499885/arma-2021-0021.pdf by The University of Utah user on 20 October 2021

[6,7] and show relatively small variation even for rather sizeable directional permeability variations. The temperature and pressure variations tend to be smoothed by the high permeability formations considered.

Relatively similar temperature-pressure profiles are shown within different layers for multi-layer reservoirs (see Figures 3-9 above), similar to a reservoir comprised of a single thick layer reservoir.

Two differences, however, are noted. First, injection and production differ for different layers, with higher injection and lower production occurring in the upper layers, as shown in Figure 12 for the four-layer model (scenario 2).

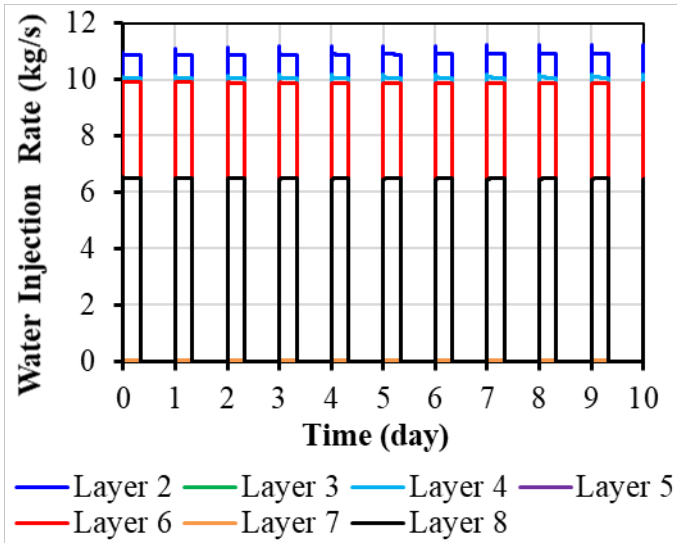

(a)

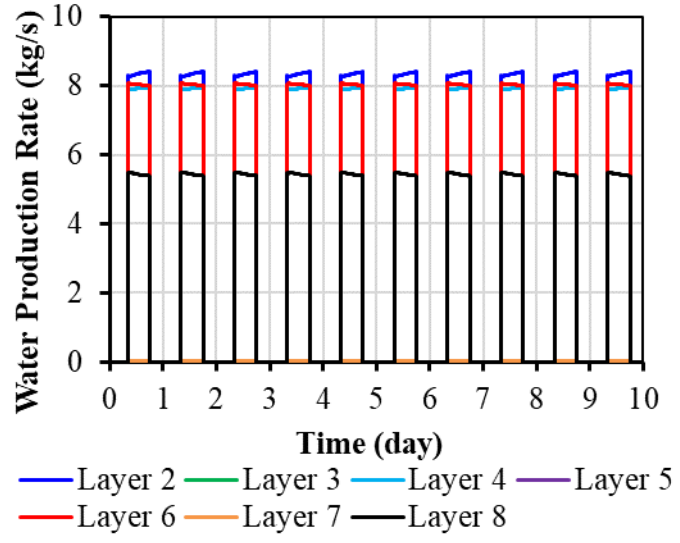

(b)

Fig. 12. (a) Injection rate and (b) production rate versus days of injection and production for the four-layer model with operational scenario 2.

The higher injection and lower production for the upper layer tend to offset each other somewhat, leading to only slightly higher temperatures in the upper layer. Additionally, the non-uniform injection-production does not appear to reduce the percent of the heat that can be recovered.

Second, for the multi-layer reservoir, the "in-between" formations (5 meters in thickness of 1 mD permeability and 5% porosity) will be heated over time differently than the high permeability-porosity reservoir layers. Heating the in-between formations can occur by hot water injection and by conduction and convection across the horizontal reservoir layer/in-between formation interface. Figure 12, however, shows that almost no hot water is injected (nor produced) from the low permeability in-between formations. Since convective heat transfer into the in-between formations is very low due to the low permeability and porosity, heat is effectively only transferred by conduction, as shown in a Figure 13.
After 120 days of injection (no production), the "in-between" formations have been heated to an average temperature of 180^{O}C (250^{O}C hot water injected into the 120^{O}C initial temperature formation).

During this heat-up of the "in-between" formations, heat recovery would be much lower than for a single thick layer reservoir if there are production cycles. However, once the "in-between" formations are heated, heat recovery for injection-production cycles becomes high, as shown in Figure 8 above, nearly 95 percent as previously reported for a single thick layer reservoir [6,7].

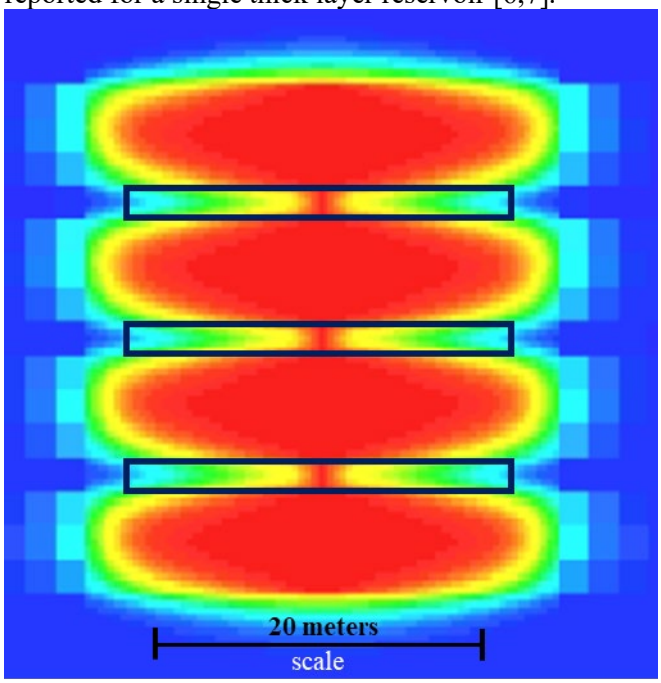

Fig. 13. Temperature profiles in the four-layer model after injection for 120 days as enlarged from Figure 3 f ("in-between" formations are outlined in black).

5. CONCLUSIONS

Downloaded from http://onepetro.org/ARMAUSRMS/proceedings-pdf/ARMA21/All-ARMA21/2499885/arma-2021-0021.pdf by The University of Utah user on 20 October 2021

High permeability and porosity deep subsurface hot water storage reservoirs in the Uinta Basin are readily available but likely as overlaying multi-layers instead of a single thick layer. Simulations were made considering two- and four-layer reservoirs and compared to a single-layer reservoir [6,7,10,13]. For multi-layer reservoir simulations, the "in-between" formations were considered to have 1 mD permeability and five percent porosity and have thicknesses of 5-meter.

Temperature and pressure profiles in the different layers of the simulated multi-layer reservoir were relatively similar to a single-layer reservoir of the same pore volume. However, injection and production tended to be somewhat unequal between all layers, with the upper layers receiving more injection and producing less. These effects somewhat offset each other, leading to only a slightly higher temperature in the upper layer.

For 1 mD permeability rock, almost no injection or production occurs into/from the "in-between" formations. Thus, the heat transfer into/from the rock is primarily by conduction across the interface boundary between the reservoir and the intervening formations. After 120 days of injecting 250^{O} C water, the initially 120^{O} C, 5-meter thick "in-between" formations have reached an average temperature of 180^{O} C. While heat recovery during the heat-up of the interbedded layers is lowered, after 120 days of injection (to "charge" the reservoir), the heat recovery is nearly 95 percent if daily injection/production cycles then occur.

Overall, the most significant effects of a multi-layer reservoir with low permeability intervening formations would seem to be the heat-up time for these intervening formations. This heat-up time will be primarily dependent on their thicknesses.

REFERENCES

Agarwal, J. C. and R. A. Giberti (2020). A Protocol for Making Renewable Energy Sizing and Selection Decisions. Power.

Andreas, O., M. Josh, A. Pau Farres, T. Alessio, R. Alessandro, L. Yongliang, D. Yulong, S. Wolf-Dieter, W. Liang, C. Haisheng and N. M. Christos (2021). "Progress and prospects of thermo-mechanical energy storage – A critical review." Progress in Energy.

Birgenheier, L. P. and M. D. V. Berg (2011). Core-based integrated sedimentologic, stratigraphic, and geochemical analysis of the oil shale bearing Green river formation, Uinta basin, Utah, DOE Award No.: DE-FE0001243.

DOE (2020). Energy Storage Grand Challenge : Draft Roadmap

Dubiel, R. F. (2003). Chapter 5: Geology, Depositional Models, and Oil and Gas Assessment of the Green River Total Petroleum System, Uinta-Piceance Province, Eastern Utah and Western Colorado. Petroleum Systems and Geologic Assessment of Oil and Gas in the Uinta-Piceance Province, Utah and Colorado.

Green, S. (2020). What Happens when the Sun Isn't Shining—Renewable Energy Storage. University of Utah Graduate Seminar, www.epirecovery.com/news.

Green, S., J. McLennan, P. Panja, K. Kitz, R. Allis and J. Moore (2021). "Geothermal battery energy storage." Renewable Energy **164**: 777-790.

Green, S., J. McLennan, P. Panja, K. Kitz, R. Allis and J. Moore (2021). Questions and Misunderstandings about the Geothermal Battery Energy Storage, www.epirecovery.com/news.

McLennan, J. and S. Green (2020). NSF Sponsored on-Line Workshop: Large-scale Subsurface Seasonal Solar Heat Storage for Future Value, University of Utah and www.epirecovery.com/news.

McLennan, J., P. Panja and S. Green (2020). Final Report-Geothermal Battery Energy Storage, NSF EAGER Grant Number 1912670 University of Utah.

Morgan, J. P. (2020). Energy Outlook 2020: Tenth Annual Energy Paper.

Panja, P., J. McLennan and S. Green (2020). Temperature and Pressure Profiles for Geothermal Battery Energy Storage in Sedimentary Basins. 54th U.S. Rock Mechanics/Geomechanics Symposium, 28 June-1 July. Golden, Colorado, American Rock Mechanics Association.

Panja, P., J. McLennan and S. Green (2021). "Influence of permeability anisotropy and layering on geothermal battery energy storage." Geothermics **90**: 101998.

Sharan, P., K. Kitz, D. Wendt, J. McTigue and G. Zhu (2020). "Using Concentrating Solar Power to Create a Geological Thermal Energy Reservoir for Seasonal Storage and Flexible Power Plant Operation." Journal of Energy Resources Technology **143**(1).

Sprinkel, D. (2016). Stratigraphy of South Flank of Uinta Mountains and Uinta Basin.

Wendt, D., H. Huang, G. Zhu, P. Sharan, J. McTigue, K. Kitz, S. Green and J. McLennan (2019). "Geologic Thermal Energy Storage of Solar Heat to Provide a Source of Dispatchable Renewable Power and Seasonal Energy Storage Capacity." GRC Transactions **43**.

Downloaded from http://onepetro.org/ARMAUSRMS/proceedings-pdf/ARMA21/All-ARMA21/2499885/arma-2021-0021.pdf by The University of Utah user on 20 October 2021